One-dimensional particle models for heat transfer analysis

2010 J. Phys.: Conf. Ser. 260 012005

(http://iopscience.iop.org/1742-6596/260/1/012005)

Journal of Physics: Conference Series **260** (2010) 012005 doi:10.1088/1742-6596/260/1/012005

One-dimensional particle models for heat transfer analysis

H Bufferand[a], G Ciraolo[a], Ph Ghendrih[b], P Tamain[b], F Bagnoli[c], S Lepri[d] and R Livi[e]

[a] M2P2, UMR 6181 - CNRS Aix-Marseille Universite - Ecole Centrale, Marseille, Technopole de Château Gombert, 38, Rue F. Joliot-Curie, 13451 Marseille, France.
[b] CEA, IRFM, 13108 St Paul-Lez-Durance, France.
[c] Dipartimento di Energetica, Università di Firenze, Via S. Marta 3, I-50139 Firenze, Italy.
[d] Instituto dei Sistemi Complessi, Consiglio Nazionale delle Ricerche, via Madonna del Piano 10, I-50019 Sesto Fiorentino, Italy.
[e] Dipartimento di Fisica, Università di Firenze, via G. Sansone 1 I-50019, Sesto Fiorentino, Italy.

E-mail: hugo.bufferand@gmail.fr

Abstract. For a better understanding of Spitzer-Härm closure restrictions and for estimating the relevancy of this expression when collisionnality decreases, an effort is done in developing simple models that aim at catching the physics of the transition from conductive to free-streaming heat flux. In that perspective, one-dimensional particle models are developed to study heat transfer properties in the direction parallel to the magnetic field in tokamaks. These models are based on particles that carry energy at a specific velocity and that can interact with each other or with heat sources. By adjusting the particle dynamics and particle interaction properties, it is possible to generate a broad range of models of growing complexity. The simplest models can be solved analytically and are used to link particle behavior to general macroscopic heat transfer properties. In particular, some configurations recover Fourier's law and make possible to investigate the dependance of thermal conductivity on temperature. Besides, some configurations where local balance is lost require defining non local expression for heat flux. These different classes of models could then be linked to different plasma configurations and used to study transition from collisional to non-collisional plasma.

1. Introduction

Heat transport in the presence of a temperature gradient imposed by heat reservoirs is a classical problem in the physics of plasmas, that has been tackled over decades by different approaches. In order to improve heat transfer modeling in weakly collisional plasma, the development of so called "toy models" is of a great interest. These models have the goal of catching the specificities of different regimes of heat transfer in the simplest way. In this paper, we focus on heat transfer in the direction parallel to the magnetic field in tokamak plasma. These plasmas are known to be weakly collisional, however, the computation of the heat flux in these plasma often relies on Spitzer-Härm expression [1] of the heat flux that is based on a strong collisionality assumption. In fact, this closure equation is used in the fluid approximation where local balance should be verified. In order to account for the departure from local balance at high temperature, the Spitzer-Härm formulation is sometime adjusted. Many examples of these flux limiter corrections

adjusting the flux expression to work at low collisionalities can be found in the literature [2; 3]. In this manuscript we aim at revisiting this problem by considering very simple models that epitomize the minimal ingredients for reproducing some general properties that are known to characterize the diffusive as well as the ballistic regimes typical of heat transfer in plasmas.

Far from a complex kinetic treatment, our models rely on particles that move along a closed magnetic field line and that exchange energy with each other. They can also interact with heat sources. In our approach, the properties of the tokamak magnetic field line are simplified and we consider that the magnetic field is constant on the field line. By comparison with a tokamak, one can consider that all the particles are passing and trapped particles are not considered. The models implemented in this work can be sorted in two categories. The first ones that will be presented in section 2 consider particles traveling with a constant velocity. The second ones illustrated in section 3 assume that particle velocities are linked to their respective energy following the relation $v = A\sqrt{E}$. We further show that these two models can be related one to another by a suitable relation.

This particle models could be studied in parallel with the kinetic treatment performed two decades ago to study transition from strongly collisional to collisionless regime [4; 5].

2. Models with constant particle velocity

The domain considered in the following model is a periodic line of length L where a heat source of energy E_{s1} is located at x_{s_1} and another one of energy E_{s2} is located at x_{s_2}. On this line, $2 \times N$ particles are uniformly spread on the mesh $\{x_i\}_{i\in[\![1,N]\!]}$, with $x_i = iL/N$. Hence, on each node of the grid x_i are located two particles. One is travelling forward with velocity v^+, one is travelling backward with velocity v^- with $|v^+| = |v^-| = v$. E_i^+ and E_i^- denote the forward $(+)$ and backward $(-)$ moving particle volumic energies, respectively. The energy $\mathcal{E}$ of a particle is given by the relation $\mathcal{E} = \mathcal{V}E = S\delta x E$, where $\mathcal{V} = S\delta x$ is the volume of a particle, S is the arbitrary surface of the particle pependicular to the direction considered so far and δx is the characteristic length of a particle equal to the mesh length $\delta x = L/N$.

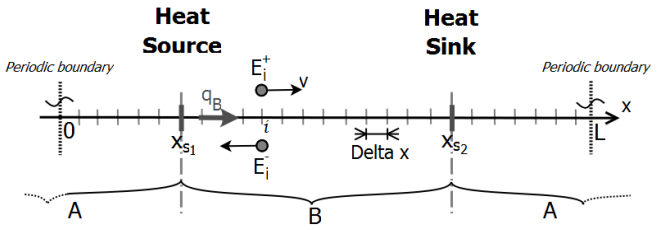

Figure 1. Sketch of the domain

The evolution law of the system relies on two steps: a *dynamic step* $(t \to t + 1/2)$ when the particles jump from one node to the closest neighboring node according to the sign of their velocity, and an *interaction step* $(t + 1/2 \to t + 1)$ during which the $+$ and $-$ particles that are located on the same node exchange part of their energy. The evolution is given by Equations 2.1 where the $t+1/2$ step is denoted with a prime and the $t+1$ step is denoted with two primes.

$$\textbf{Dynamic step} \qquad \begin{cases} E_i^{+\prime} &= E_{i-1}^{+} \\ E_i^{-\prime} &= E_{i+1}^{-} \end{cases} \qquad\qquad \textbf{Interaction step} \qquad \begin{cases} E_i^{+\prime\prime} &= E_i^{+\prime} + \frac{E_i^{-\prime} - E_i^{+\prime}}{\alpha} \\ E_i^{-\prime\prime} &= E_i^{-\prime} + \frac{E_i^{+\prime} - E_i^{-\prime}}{\alpha} \end{cases} \tag{2.1}$$

α is a number that quantify the exchanged amount of energy between the particles. If $\alpha = 2$, the energy of the two particles after the interaction is the same. In this case, one can say that the

interaction is total. Moreover, when the particles pass through the nodes $x_{i_{s1}}$ and $x_{i_{s2}}$ where the heat sources are located, they take the energy of the source. In stationary conditions, we have for all i, $E_i^{\pm\prime\prime} = E_i^{\pm}$. Hence, using Equations (2.1), the solution can be obtained by iterating equations (2.2) with the "boundary conditions" $E_{i_{s1}}^{\pm} = E_{s1}$ and $E_{i_{s2}}^{\pm} = E_{s2}$.

$$\left\{ \begin{array}{rcl} E_i^+ & = & E_{i-1}^+ + \Delta E_i \\ E_i^- & = & E_{i+1}^- - \Delta E_i \end{array} \right. \quad \text{with} \quad \Delta E_i = \frac{E_{i+1}^- - E_{i-1}^+}{\alpha} \tag{2.2}$$

From recursive serie analysis, one can prove that the solution takes the form $E_i^+ = ai + b$ and $E_i^- = ci + d$. Reporting these expressions in Equations 2.2 and considering the boundary conditions, one obtains the value of a, b, c and d:

$$\left\{ \begin{array}{rcl} E_i^+ & = & \frac{E_{s1}-E_{s2}}{i_{s1}-i_{s2}+(2-\alpha)} \cdot i + \frac{E_{s2}\cdot i_{s1} - E_{s1}\cdot i_{s2} + E_{s1}\cdot(2-\alpha)}{i_{s1}-i_{s2}+(2-\alpha)} \\ E_i^- & = & \frac{E_{s1}-E_{s2}}{i_{s1}-i_{s2}+(2-\alpha)} \cdot i + \frac{E_{s2}\cdot i_{s1} - E_{s1}\cdot i_{s2} + E_{s2}\cdot(2-\alpha)}{i_{s1}-i_{s2}+(2-\alpha)} \end{array} \right. \quad \text{for } i \in [\![i_{s1}, i_{s2}]\!] \tag{2.3}$$

It is also possible to compute the energy exchanged with the source at each time step. For instance, for source s_1, this energy increment is given by the relation

$$\delta\mathcal{E} = \mathcal{V} \cdot \left(2E_{s1} - E_{i_{s1}}^{+\prime} - E_{i_{s1}}^{-\prime} \right) = \mathcal{V} \left(2E_{s1} - E_{i_{s1}-1}^{+} - E_{i_{s1}+1}^{-} \right) \tag{2.4}$$

Also, since $E_{s1} = E_{i_{s1}}^- = E_{i_{s1}}^+$, the expression of the $\delta\mathcal{E}$ can be expressed as

$$\delta\mathcal{E} = \mathcal{V} \cdot \left\{ (E_{i_{s1}}^- - E_{i_{s1}-1}^+) + (E_{i_{s1}}^+ - E_{i_{s1}+1}^-) \right\} \tag{2.5}$$

One notices from Equation 2.2 that the quantity $\xi_i = E_{i-1}^+ - E_i^-$ verifies $\xi_{i+1} = \xi_i = \xi$. This quantity is conserved wherever the particles interact with each other and do not interact with the sources. These subdomains are denoted with the letter A and B on Figure 1. Consequently, the energy exchanged with the source s_1 can also be written as $\delta E = \mathcal{V}(-\xi_A + \xi_B)$. If we divide this energy by the time step $\delta t = \delta x / v$ and by the surface S, one can determine the heat flux q by

$$q = \frac{\delta\mathcal{E}}{S \cdot \delta t} = v(-\xi_A + \xi_B) = q_A + q_B \tag{2.6}$$

Using Equations 2.3 gives the following expression for q_B

$$q_B = v \cdot \xi_B = v(E_{i_{s1}}^+ - E_{i_{s1}+1}^-) = v \cdot \frac{(E_{s1} - E_{s2})\,(1-\alpha)}{i_{s1} - i_{s2} + (2-\alpha)} \tag{2.7}$$

Besides, one can calculate the energy gradients,

$$\nabla E^{\pm} = \frac{E_{i+1}^{\pm} - E_i^{\pm}}{x_{i+1} - xi} = \frac{1}{\delta x} \cdot \frac{E_{s1} - E_{s2}}{i_{s1} - i_{s2} + (2-\alpha)} \tag{2.8}$$

Reporting equation 2.8 into Equation 2.7 gives

$$q_B = -(\alpha - 1) \cdot \delta x \cdot v \cdot \nabla E^{\pm} \tag{2.9}$$

As noticed previously, the case where $\alpha = 2$ is of particular interest since it implies a thermalization between the $+$ and $-$ particles. This condition guarantees local equilibrium, i.e. $E_i^+ = E_i^-$. This balance leads to defining the temperature as $T \sim E^{\pm}$. The heat flux is then expressed by the standard Fourier law for heat conduction : $q = -v\delta x \nabla T = -\kappa \nabla T$. Moreover, this expression is compatible with the standard derivation of heat conductivity [6]:

$$\kappa = k_B n \lambda v_{th} \tag{2.10}$$

where λ is the mean free path, v_{th} is the thermal speed, k_B is Boltzmann constant and n is the plasma density. In the case where $\alpha = 2$, the equivalent mean free path is δx since thermalization occurs at the lattice scale. v plays the role of the thermal speed.

For $\alpha \neq 2$, $E_i^+ \neq E_i^-$ and it is not possible to define local balance at the mesh scale. However, if we define $\bar{E} = (E^+ + E^-)/2$, we have a Fourier's like expression for the heat flux that is $q = -v(\alpha - 1)\delta x \, \nabla \bar{E}$. In this case, we have $\kappa = v(\alpha - 1)\delta x$. To be coherent with the usual derivation of heat capacity, one should find that the equivalent mean free path in this case is $\lambda = (\alpha - 1)\delta x$. In fact, the interaction rule guarantees an exponential decay to equilibrium after a characteristic number of interactions $n = \alpha - 1$ and thus a characteristic decay length compatible with the above expression for the mean free path.

For α going to infinity, the + and − particles almost do not interact with each other. A standard collisionless regime is then expected. Indeed, using Equations 2.3, one can find directly that $\nabla E^{\pm} \to 0$. Hence, in the domain B of Figure 1 for instance, we have $E_{s1} = E^+ \neq E^- = E_{s2}$ and there is no local equilibrium. As expected, the mean free path tends to infinity and the particle behavior is ballistic. Moreover, making $\alpha \to \infty$ in Equation 2.7 gives $q = v(E_{s1} - E_{s2})$ which is compatible with the ballistic expression of heat flux.

On Figure 2 are plotted results for $\alpha = 2$ and $\alpha = 30$. In the first case, one can notice that $E^+ = E^- = \bar{E}$ that defines local equilibrium.

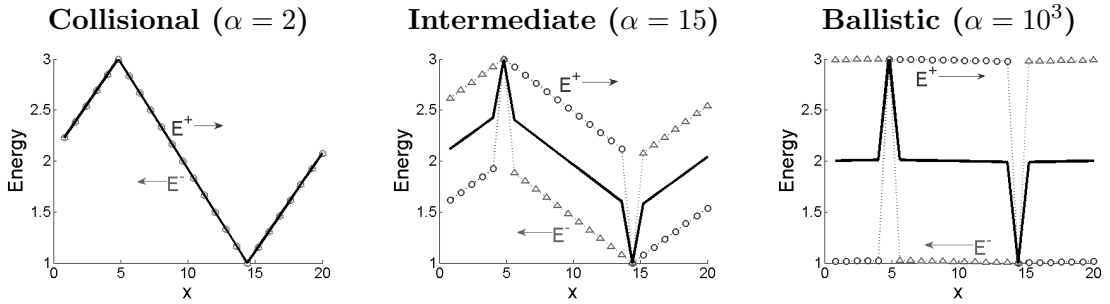

Figure 2. Simulations performed with constant velocity for different values of α. E^+ (circles), E^- (triangles) and $\bar{E}$ (solid thick line). The sources are located at $x = 5$ and $x = 15$. Their respective energies are 3 and 1. The length of the domain is 20. The number of particles is 2×50

To go further, since the quantity $\lambda = (\alpha - 1)\delta x$ plays the role of mean free path, it can be interesting to introduce also a dependance of α on the energy. This is done by considering the following law for α:

$$\alpha_i = 2 \cdot \left(\frac{\max(E_i^+, E_i^-)}{E_{\text{ref}}} \right)^r \tag{2.11}$$

In this expression, E_{ref} is chosen small enough to ensure that the energy ratio is always larger than one such that $\alpha > 2$. r is a positive real number. The idea is to consider the case where $\alpha \gg 1$ yielding the approximation $\lambda = \delta x(\alpha - 1) \approx 2\delta x \left(\max(E_i^+, E_i^-)/E_{\text{ref}}\right)^r \propto {E_i}^r$. For plasma physics, the case where $r = 2$ is of particular interest since Coulombian interactions between plasma particles give a mean free path proportional to the energy square. The assumption $\alpha \gg 1$ does not imply that collisionless cases are the only ones considered. Indeed, as long as $\lambda \ll L \Leftrightarrow (\alpha - 1) \ll N$ where L is the domain legnth anf N the number of interactions undergone by a particle as it travels through the domain, the model can be supposed to be collisional.

We are interested in finding analytical solutions for this system. We will solve it in the domain

B on Figure 1 where $E^+ > E^-$. The system to solve is then

$$\left\{ \begin{array}{rcl} E_i^+ & = & E_{i-1}^+ + \frac{E_{i+1}^- - E_{i-1}^+}{2\cdot(E_{i-1}^+/E_{\rm ref})^r} = E_{i-1}^+ + \varepsilon \cdot (E_{i+1}^- - E_{i-1}^+) \\ E_i^- & = & E_{i+1}^- - \frac{E_{i+1}^- - E_{i-1}^+}{2\cdot(E_{i-1}^+/E_{\rm ref})^r} = E_{i+1}^- - \varepsilon \cdot (E_{i+1}^- - E_{i-1}^+) \end{array} \right. \tag{2.12}$$

where $\varepsilon = 1/\alpha \ll 1$. One must notice that the numerator of the exchange term can be developped as

$$\begin{array}{rcl} E_{i+1}^- - E_{i-1}^+ & = & E_{i+1}^- - E_i^+ + (E_i^+ - E_{i-1}^+) \\ & = & E_{i+1}^- - E_i^+ + \varepsilon \cdot (E_{i+1}^- - E_{i-1}^+) \\ & \approx & E_{i+1}^- - E_i^+ = \xi = \text{constant} \end{array}$$

Hence, the problem is reduced to solving recursive Equation 2.13 for E_i^+:

$$E_i^+ = E_{i-1}^+ + \frac{B}{(E_{i-1}^+)^r} \quad \text{with} \quad B = \xi \cdot E_{\rm ref}^r/2 \tag{2.13}$$

An approximate solution is

$$E_i^+ = \left(E_{s1}^{1+r} + (i - i_{s1}) \cdot B \cdot (1+r)\right)^{\frac{1}{1+r}} \tag{2.14}$$

The unknown B is determined using $\xi = E_i^- - E_{i-1}^+ = 2B/E_{\rm ref}^r$ and $E_{i_{s2}}^- = E_{s2}$. Reporting in Equation 2.14 for $i = i_{s2} - 1$, one find

$$2B/E_{\rm ref}^r = E_{s2} - \left(E_{s1}^{1+r} + (i_{s2} - 1 - i_{s1}) \cdot B \cdot (1+r)\right)^{\frac{1}{1+r}} \tag{2.15}$$

Solving equation 2.15 gives B, ξ and finally the heat flux q. The simulation results are compared with the analytical solution on Figure 3. One expects to find a good agreement between the simulation results and the analytical solution in the cases where $\alpha \gg 1$. For the first case, we have chosen $E_{\rm ref} = 0.5$, $E \in [2,\ 5]$ and $r = 2$ hence $\alpha \in [16,\ 100] \gg 1$. The hottest particles will thus require about 100 interactions to thermalize. The number of particles used in the simulation is $N = 2 \times 3000$. Consequently, each particle undergoes 3000 interactions when it covers the domain. Since $3000 \gg 100$, this case can then be considered as a collisional case, that is $\lambda \ll L$. In fact, on Figure 3,a, one can notice that for all i, $E_i^+ \approx E_i^-$. In the second case, we choose the same parameters except that we limit the number of particles to 300. Thus, the relation $\lambda \sim L$ applies and the case is not collisional. One can notice the departure between E^+ and E^- on Figure 3,b

3. Models with non-constant velocity

Unlike the previous models where the velocity of particles is constant, a dependancy of velocity on the energy is added such that $v^\pm = A\sqrt{E^\pm}$. The previous energy can now be seen as the particle's kinetic energy. In the following simulations, we consider the same domain as described on Figure 1. Particles are randomly placed in the domain with a given initial energy. One half is moving forward and one half is moving backward. The algorithm detects when two particles meet or when they meet the sources. In that case, particles exchange part of their energy with the same rules as those described in the previous section. The particle's velocity modules are recalculated and their velocity sign is conserved. Since the sign of velocity is unchanged, particles exchange energy with the two source alternatively. The U-turn is not allowed since making the

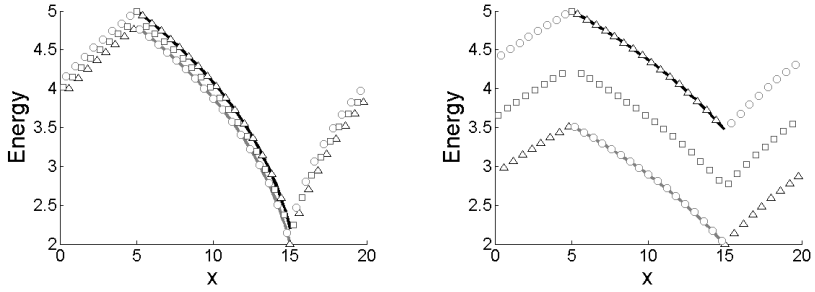

(a) (b)

Figure 3. Simulation results with $\alpha \propto \max(E^+, E^-)^2$. $E_{s_1} = 5$ and $E_{s_2} = 2$. (a): Energy profiles obtained when the simulation is performed with 2×3000 particles and guarantee that for all i, $1/\alpha \ll 1$ and $\lambda \ll L$. (b): The simulation is performed with 2×300 particles for $\lambda \sim L$. Simulations results are plotted with symbols: E^+ (triangles), E^- (circles) and $\bar{E}$ (squares). Analytical estimations corresponding to Equation (2.14) are plotted with lines.

two traveling directions equally probable would lead to defining an automatic local equilibrium. As a consequence, some fluctuations apart, the rate of interaction with the two sources is the same. This interaction rate is also characteristic of the rate with which particles interact with each other. Analytical solutions are more difficult to obtain for this kind of model since there is no well defined lattice for solving the recursive equations. However, in the collisional case where $E^+ \approx E^-$, an approximate solution can be found by solving Equations (2.1,2.12) on the lattices $\{x_i^+\}$ and $\{x_i^-\}$, see Figure 4, where

$$\begin{cases} |x_{i+1}^+ - x_i^+| &= |\delta t \cdot v_i^+| = \delta t \cdot A\sqrt{E_i^+} \\ |x_i^- - x_{i-1}^-| &= |\delta t \cdot v_i^-| = \delta t \cdot A\sqrt{E_i^-} \end{cases} \tag{3.1}$$

Since $E_i^+ \approx E_i^-$, one has $\forall i,\ \Delta x_i^+ \approx \Delta x_{i-1}^-$ and one can define the lattice $x_i \sim x_i^+ \sim x_i^-$, see Figure 4. To determine the values of x_i for all i, one has to solve $\Delta x_i = A\delta t\sqrt{E_i}$ constrained by $\sum_N \Delta x_i = L$ where the values of E_i are given by the solutions found in the previous section. One has to remember that this approach is only valid for the collisional cases.

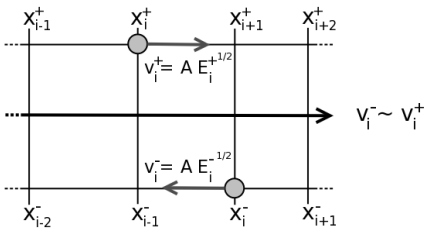

Figure 4. Lattice definitions in the collisional approximation for non-constant velocity

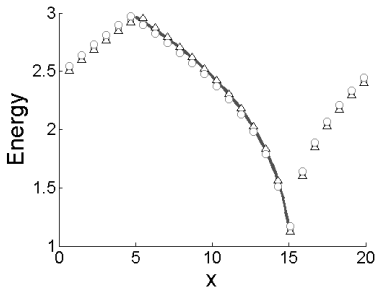

Figure 5. Energy profiles in the non-constant velocity case for $r = 2$. Simulation results: E^+ (triangles), E^- (circles) and $\bar{E}$ (squares). Line: analytical estimation. Number of particles: 2×500.

In particular, one finds $\{x_i\}$ in the case where the mean free path depends on the energy. From Equation 2.14, the energy is given by the relation

$$E_i = (a + b \cdot i)^{1/(1+r)} \tag{3.2}$$

where $a = E_{s_1}^{1+r} - Bi_{s_1}(1+r)$ and $b = B(1+r)$. In the following, we just focus on the domain B defined on Figure 1. In order to determine the value of x_i, we use the approximation $\Delta x_i/\Delta i \approx \mathrm{d}x/\mathrm{d}i$. Hence,

$$\begin{array}{rcl} \mathrm{d}x & = & A\delta t(a+b\cdot i)^{\frac{1}{2(1+r)}}\,\mathrm{d}i \\ x_i - x_{s1} & = & A\delta t \int_{i_{s1}}^{i}(a+b\cdot i)^{\frac{1}{2(1+r)}}\,\mathrm{d}i \\ x_{s2} - x_{s1} & = & A\delta t \int_{i_{s1}}^{i_{s2}}(a+b\cdot i)^{\frac{1}{2(1+r)}}\,\mathrm{d}i \end{array} \tag{3.3}$$

The solution of these equations is

$$\left\{ \begin{array}{rcl} x_i & = & c + d(a+b\cdot i)^{\frac{3+2r}{2(1+r)}} \\ i & = & \frac{1}{b}\left(\frac{x_i - c}{d}\right)^{\frac{2(1+r)}{3+2r}} - \frac{a}{b} \end{array} \right. \tag{3.4}$$

c and d can be determined using $x_{i_{s1}} = x_{s_1}$ and $x_{i_{s2}} = x_{s_2}$. Reporting the expression of i in Equation 3.2 gives

$$E_i = \left(\frac{x_i - c}{d}\right)^{\frac{2}{3+2r}} \tag{3.5}$$

Since in the collisional case, one has $E(x_{s1}) = E_{s1}$ and $E(x_{s2}) = E_{s2}$, the constant can be determined and the energy is finally given by Equation 3.6.

$$E = \left(E_{s1}^{1/\beta} + \frac{E_{s2}^{1/\beta} - E_{s1}^{1/\beta}}{x_{s2} - x_{s1}}(x - x_{s1})\right)^{\beta} \qquad \text{with} \qquad \beta = \frac{2}{3+2r} \tag{3.6}$$

In this collisional case where a lattice has been determined, the heat flux can be calculated as in the previous section, see Equation 2.7. The velocity is now a function of the temperature:

$$\begin{array}{rcl} q & = & \frac{\mathcal{V}\cdot(E_i^+ - E_{i+1}^-)}{S\cdot\delta t} = \ell\cdot A\sqrt{E_i}\frac{E_i^+ - E_i^-}{x_{i+1}-x_i} \\ & = & -A\cdot\ell\cdot(\alpha-1)\sqrt{\bar{E}}\nabla\bar{E} \end{array} \tag{3.7}$$

On Figure 5, a comparison between simulation results in the collisional case for $r = 2$ and the above analytical estimation is plotted. The $+$ and $-$ particles energy are shown. One notices that these two variables are almost equal which justifies the above approximations.

We also study the dependance of the heat flux on the energy in the case $r = 2$. To do so, the number of particles is kept constant equal to 500. The energy of the source is chosen as $E_{s_1} = 1.05 \times E_0$ and $E_{s_2} = 0.95 \times E_0$ where E_0 is a parameter that describes the energy of the system. We choose $E_{\mathrm{ref}} = 0.8$ and simulations are performed for values of E_0 between 2 and 200. A particle undergoes approximately $N_{\mathrm{inter}} = 500$ interactions as it travels from one source to the other. Since α represents the number of interactions necessary to thermalize, the regime is expected to be collisional for $\alpha = 2(E_0/E_{\mathrm{ref}})^2 < 500$. To make it clearer, we define the collisionality ν^* as $\nu^* = N_{\mathrm{inter}}/\alpha$. We are in a collisional regime if $\nu^* > 1$ that is $E_0 < 13$. For $E_0 > 13$, the regime is ballistic. The distance between the source is denoted $\mathcal{L}$. For each case, one computes the average gradient of $\bar{E}$. On Figure 6,a is plotted the equivalent heat condictivity $\kappa = q/\bar{E}$ as a function of E_0. On Figure 6,b is plotted $q\mathcal{L}/(E_{s_1} - E_{s_2})$.

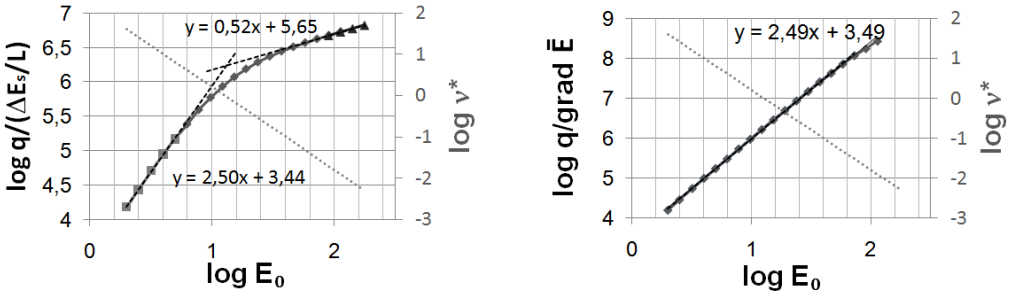

(a) (b)

Figure 6. (a). $q/\{(E_{s_1} - E_{s_2})/L\}$ as a function of the energy of the system E_0. Simulation results (symbols) exhibiting the transition from conductive to ballistic regime. Power law fittings are represented with lines. (b). Effective heat conductivity $\kappa = q/\nabla \bar{E}$ as a function of the energy of the system E_0, simulation results (symbols), power law fitting (line) exhibiting $\kappa \propto E_0^{5/2}$. The collisionality is plotted with dot-line.

On Figure 6,a we notice that for low energies we have $q \propto E_0^{5/2}(E_{s2} - E_{s1})/\mathcal{L}$. Besides, for low energies, we have $\nabla T \approx (E_{s_2} - E_{s_1})/\mathcal{L}$ thus $q \propto E_0^{5/2}\nabla T$. This characteristic of the collisional Spitzer-Härm regime. For high energy, we have $q \propto \sqrt{E_0}(E_{s_2} - E_{s_2})/\mathcal{L} \sim v_{th}(E_{s_2} - E_{s_2})$. This is characteristic of the ballistic regime. The transtion occurs for $\nu^* = 1$, as expected. On Figure 6,b we notice that with the definition of $\bar{E} = (E^+ + E^-)/2$, we recover the Spitzer-Härm like law for the heat flux, even in the collisionless case ($\nu^* < 1$).

4. Conclusions

The analysis of simple models where energy transfer takes place exhibits the well-known Spitzer-Härm diffusive behavior in the collisional regime. Also, the transition from collisional to ballistic behavior was observed as the equivalent mean free path of the particles increased. This transition can be compared with the one observed with a kinetic treatment limited to considering 4 moments of the distribution function [4; 5]. In the present "toy-model", no distinction is made between thermal and suprathermal particles. A perspective of this work could be to introduce this ingredient to investigate flux-limiter formulations that are used when thermal particles are collisional and suprathermal particles are ballistic.

Acknowledgements

This work supported by the ANR project ESPOIR and by the European Communities under the contract of Association between EURATOM and CEA, was carried out within the framework of the European Fusion Development Agreement. The views and opinions expressed herein do not necessarily reflect those of the European Commission.

References

[1] Spitzer L and Härm R 1953 *Phys. Rev.* **89-5**
[2] Luciani J F and Mora P 1983 *Phys. Rev. Lett.* **51** 1664–1667
[3] Fundamenski W 2005 *Plasma Phys. Control. Fusion* **47** R163–R208
[4] Bond D J 1981 *J. Phys. D: Appl. Phys.* **14**
[5] Shirazian M H and Steinhauer L C 1981 *Phys. Fluids* **24**
[6] Stangeby P C 2000 *The Plasma Boundary of Magnetic Fusion Devices* (IoP)